Energy-Consistent Pseudopotentials for the 5d Elements—Benchmark Calculations for Oxides, Nitrides, and Pt_2[†]

Benjamin Spohn, Erich Goll, and Hermann Stoll*

Institut für Theoretische Chemie, Universität Stuttgart, D-70550 Stuttgart, Germany

Detlev Figgen

Centre for Theoretical Chemistry and Physics, New Zealand Institute for Advanced Study, Massey University Albany, Auckland 0745, New Zealand

Kirk A. Peterson

Department of Chemistry, Washington State University, Pullman, Washington 99164-4630

Received: April 17, 2009; Revised Manuscript Received: June 17, 2009

The performance of new relativistic energy-consistent pseudopotentials for the 5d elements, adjusted to atomic valence spectra from multiconfiguration Dirac−Hartree−Fock calculations (*J. Chem. Phys*. **2009**, *130*, 164108.), is examined in coupled cluster and multireference configuration interaction benchmark calculations for the diatomics HfO, TaO, WO, ReN, OsN, IrN, and Pt_2, with basis sets of up to quintuple-ζ quality. The final accuracy reached for the oxides and nitrides, with corrections for pseudopotential errors (contributions from 4f shell correlation, for example), is 0.3 pm for bond lengths and 17 cm^{-1} (1.5%) for harmonic vibrational frequencies. The spectroscopic constants of the ground state of Pt_2 can be reproduced with deviations of 3 pm for the bond length and 1 cm^{-1} for the vibrational frequency, without any correction for pseudopotential errors.

1. Introduction

Pseudopotentials (PPs) are used in quantum chemistry to relieve ab initio calculations of heavy-atom compounds from the computational burden of explicitly treating large, chemically inactive cores; they also allow for an inexpensive, implicit treatment of relativistic effects.[1,2] Of course, there is a price to pay with respect to the accuracy of the results: The frozen-core approximation is involved, there are changes in the nodal structure of the valence orbitals, and a semilocal one-center/one-electron representation of the potential is used, etc. In the case of the energy-consistent PPs, see, for example, refs 3 and 4, these approximations already leave their fingerprint, in the form of fitting errors, when adjusting the PP atomic valence spectra to all-electron reference data. Moreover, as for other kinds of PPs, there are transferability errors when applying the PPs to molecules (and/or to theoretical levels different from that used in the adjustment procedure). Benchmark calculations revealing the size of the latter errors are not only important per se, that is, to estimate the size of the errors to be expected in the application of the PPs, but are essential also as indicators of how to further improve the PPs.

Within the present paper, we report benchmark calculations of this kind for our newly generated set of energy-consistent PPs for the row of 5d elements.[5] These PPs were fitted, at the two-component level, to atomic valence spectra from four-component all-electron multiconfiguration Dirac−Hartree−Fock (MCDHF) calculations. They are of the small-core variety, that is, the valence 6s5d electrons are treated explicitly together with the outer-core 5sp orbitals; this guarantees a good spatial and energetic separation between valence/outer-core and the inner core simulated by the PPs and has been recognized as instrumental for achieving high PP accuracy. In fact, we could reach an accuracy of 0.01 eV for averages of orbital configurations and of 0.05 eV for individual relativistic states in our fit to the atomic valence spectra of the row of 5d elements. Note that the present generation of energy-consistent MCDHF-adjusted PPs goes back to a pilot study[6] performed in cooperation with Prof. R. M. Pitzer.

For their use in quantum-chemical codes, our new 5d PPs are accompanied by series of correlation-consistent polarized valence n-ζ (cc-pVnZ-PP) basis sets of the Dunning type,[7,5] optionally with additional diffuse functions (aug-cc-pVnZ-PP) and/or functions for correlating the outer-core shells [(aug-)cc-pwCVnZ-PP]. It is only with such series of basis sets (which up to now are unique to our energy-consistent PP) that one is able, by means of basis set extrapolation, to separate basis set deficiencies from intrinsic PP errors.

PPs and accompanying basis sets are used in the present work to calculate ground-state potential energy curves for the 5d monoxides HfO, TaO, and WO and the mononitrides ReN, OsN, and IrN. These molecules were chosen because reliable experimental data are available for them in the literature.[8−13] We calculate equilibrium bond lengths r_e, harmonic vibrational frequencies ω_e, and dissociation energies D_e. In each case, we monitor basis set effects, as well as the influence of valence and core−valence correlation. We also make comparison to relativistic all-electron calculations and study the contribution of correlation effects of the energetically high-lying 4f shell. Moreover, scalar-relativistic calculations are supplemented by two-component ones, to reveal the influence of spin−orbit (SO) interaction. Having thus analyzed the reliability of our PPs, we

[†] Part of the "Russell M. Pitzer Festschrift".

10.1021/jp903543f CCC: $40.75
Published on Web 07/10/2009

employ them for an investigation of the electronic spectrum of the platinum dimer, Pt_2.

The paper begins with a section on computational details; the main sections (sections 3 and 4) contain the results of our calculations and their discussion, and section 5 concludes with a short summary.

2. Computational Details

We performed calculations for the potential curves of the HfO, TaO, WO, ReN, OsN, and IrN ground states. The PP calculations used the PP parameters and accompanying cc-pVnZ-PP and cc-pwCVnZ-PP basis sets from ref 5 for the 5d elements and aug-cc-pVnZ basis sets[14,15] for O and N. First, a series of restricted open-shell coupled-cluster calculations with single and double excitations and perturbative account of triples [RCCSD(T)[16−19]] based on restricted open-shell HF reference wave functions were done, correlating the valence 6s5d metal and 2sp O, N shells and using the valence triple-, quadruple-, and quintuple-ζ basis sets; subsequently, the results were extrapolated to the basis set limit (CBS) for each point of the potential curve. Next, similar calculations were performed including metal outer-core−valence correlation, that is, adding the metal 5sp orbitals to the correlated space and using the cc-pwCVnZ-PP basis sets for the metals.

To monitor the multireference character of the diatomics under consideration, we supplemented the CCSD(T) calculations by complete-active-space self-consistent-field (CASSCF[20,21]) and multireference configuration interaction ones with single and double excitations (MRCISD[22,23]), including the Davidson correction[24] in the latter case. In these calculations, all metal 6s5d and N, O 2sp orbitals were included in the active space, but the metal 5sp orbitals were kept doubly occupied in the CASSCF and were not correlated in the MRCISD; triple-ζ basis sets were used.

For IrN and OsN, we also checked the influence of full triple and quadruple excitations at the coupled cluster level (CCSDT and CCSDTQ[25]), using triple- and double-ζ basis sets, respectively; again, only valence (metal 6s5d, O, N 2sp) correlation was included.

SO effects were evaluated by calculating, at the MRCISD level, matrix elements of the SO part of the PP[5] between ground and low-lying correlated states and subsequently diagonalizing the resulting matrix. The diagonal elements were shifted with the difference between the best coupled cluster ground-state energies [CBS, CCSD(T) including core−valence correlation] and the corresponding MRCISD ones.

To check the accuracy of the PP calculations, we also performed RCCSD(T) all-electron (AE) calculations with the third-order Douglas−Kroll−Hess (DK3) Hamiltonian,[26,27] using basis sets of triple-ζ quality. For this purpose, specially optimized cc-pwCVTZ-DK3 all-electron basis sets[5] were applied in calculations with/without outer-core correlation. Additional high-l basis functions were included for discussing the influence of correlation effects originating from the energetically high-lying closed 4f shell (cc-pwCVTZ-DK3+4f).[5] Differential basis-set superposition errors (BSSE), that is, the BSSE for the 4f correlation effects, are quite small with this basis; for ReN, they amount to 0.04 pm for r_e, ∼0.2 cm^{-1} for ω_e, and ∼0.2 kcal/mol for D_e.

To explore the best possible description of Pt_2, we first investigated its electronic spectrum at the scalar-relativistic level. For this purpose, we employed CCSD(T) calculations, including outer-core correlation, using the series of cc-pwCVnZ basis sets with extrapolations of the energies to the basis set limit. As excited low-spin, that is, singlet, states cannot be treated in CCSD(T) calculations, the CCSD(T) energy of such a state with symmetry Λ was simulated using $E^{CC}(^1\Lambda) = E^{CI}(^1\Lambda) + E^{CC}(^3\Lambda) - E^{CI}(^3\Lambda)$, that is, by shifting the CI energy $E^{CI}(^1\Lambda)$ of this state by the energy difference between the coupled cluster energy $E^{CC}(^3\Lambda)$ and the CI energy $E^{CI}(^3\Lambda)$ of the triplet state with the same orbital occupation. A similar problem arises for the $^3\Phi_u$ and $2^3\Pi_u$ states as well as for the $^3\Gamma_u$ and $^3\Sigma_u^+$ states: In both cases, both triplet states arise from the same orbital occupation; therefore, a single-reference treatment of a state with this orbital occupation describes the average over both states. The energy splitting between both states has been evaluated at the MRCISD level using the cc-pwCV5Z basis set; the final coupled cluster energy $E^{CC}(i)$ for an individual state i then is simulated as $E^{CC}(i) = E^{CC}(\text{av}) + E^{CI}_{MR}(i) - E^{CI}_{SR}(\text{av})$. As the single-reference CI energy $E^{CI}_{SR}(\text{av}) \neq 0.5[E^{CI}_{MR}(i) + E^{CI}_{MR}(j)]$, a small error is introduced due to this energy shift; nevertheless, even in the case of the $^3\Phi_u$ and $2^3\Pi_u$ states, which show an energy splitting of ∼2000 cm^{-1}, this error amounts to only ∼20 cm^{-1} for the energies and is completely negligible for the determination of r_e and ω_e. In all cases, the orbitals were optimized in RHF or state-specific MCSCF calculations and fully symmetry adapted.

The scalar-relativistic coupled cluster energies at the basis set limit serve as diagonal elements in our SO treatment of Pt_2. Although we aim to describe the lowest relativistic levels, we want to include as much of the SO coupling between scalar-relativistic states as possible, and the SO matrix was therefore built from all scalar-relativistic states apart from the very high $2^1\Delta_g$ and $^1\Sigma_u^+$ states. The orbitals were averaged in a MCSCF calculation for all states, and the off-diagonal elements of the initial SO matrix were evaluated at the MRCISD level using the cc-pVQZ basis.

All calculations were done using the MOLPRO suite of ab initio programs.[28] Points of the potential curves were determined in equidistant increments of 0.03 Å and were least-squares fitted by a function $\Sigma_{i=-1}^{4} a_i r^i$, from which equilibrium bond lengths (r_e) and harmonic frequencies (ω_e), as well as equilibrium total energies (E_e) for evaluating dissociation energies D_e and term energies T_e, were extracted. No counterpoise correction was applied, that is, $E^{at}(M) + E^{at}(X) - D_e = E_e$, where the atomic energies E^{at} of the metal M and the N, O atoms were calculated with one-center basis sets only. All dissociation energies of the present work were evaluated with respect to neutral ground-state atoms.

3. Results for Nitrides and Oxides

In this section, we discuss results for bond lengths (r_e), harmonic vibrational frequencies (ω_e), and dissociation energies (D_e), with respect to ground-state atoms, of the diatomics HfO ($1\sigma^2 2\sigma^2 1\pi^4 1\delta^n 3\sigma^2$ configuration with $n = 0$, $^1\Sigma^+$ ground state), TaO ($n = 1$, $^2\Delta_{3/2}$), WO [$n = 2$, $^3\Sigma^-$ (0^+)], ReN [$n = 2$, $^3\Sigma^-$ (0^+)], OsN ($n = 3$, $^2\Delta_{5/2}$), and IrN ($n = 4$, $^1\Sigma^+$). Let us start from scalar-relativistic PP calculations at the CCSD(T) level and discuss various contributions to the above properties, their sensitivity to computational parameters, and possible corrections; see Tables 1−3.

3.1. Basis Set Effects. We performed calculations with the series of cc-pVnZ-PP and cc-pwCVnZ-PP basis sets ($n = 3-5$) for the metal atoms, in the latter case also correlating the metal outer-core 5sp shells. In both cases, we extrapolated to the CBS using the SCF energies from $n = 5$ and a $1/n^3$ ansatz[36] (using $n = 4, 5$) for the basis set dependence of the correlation energies. The total effect of basis set enlargement (cc-pVTZ → CBS, cc-pwCVTZ → CBS) is listed in Tables 1 (r_e), 2 (ω_e), and 3

TABLE 1: Analysis of Various Contributions to Bond Lengths r_e (pm)[a]

	HfO	TaO	WO	ReN	OsN	IrN
basis set effect vtz→CBS	−0.381	−0.466	−0.521	−0.677	−0.634	−0.582
basis set effect wcvtz→CBS	−0.762	−0.759	−0.727	−0.701	−0.586	−0.460
valence correlation	4.812	4.148	3.931	5.693	5.271	4.825
5sp correlation	−2.682	−1.676	−1.065	−0.445	−0.134	0.073
PP error, SCF	−1.771	−0.937	−0.553	−0.427	−0.229	−0.135
PP error, SCF+CCSD(T), val	−1.845	−1.216	−0.728	−0.425	−0.327	−0.235
PP error, SCF+CCSD(T), val+5sp	−1.966	−1.325	−0.785	−0.467	−0.336	−0.235
4f correlation	−0.954	−0.713	−0.543	−0.450	−0.335	−0.273
effect of triples	1.243	1.387	1.534	1.900	1.818	1.726
MRCISD vs CCSD(T)	−0.023	−0.021	0.011	0.527	0.488	0.562
SO	0.000	0.045	0.051	−0.042	0.156	0.552

[a] For a detailed explanation, see the text.

TABLE 2: Analysis of Various Contributions to Harmonic Wavenumbers ω_e (cm^{-1})[a]

	HfO	TaO	WO	ReN	OsN	IrN
basis set effect vtz→CBS	3.16	5.36	7.18	12.39	10.20	8.85
basis set effect wcvtz→CBS	11.81	11.25	10.18	13.65	10.78	5.75
valence correlation	−102.12	−108.19	−121.07	−192.61	−184.31	−160.77
5sp correlation	39.60	19.78	15.91	10.81	5.68	2.86
PP error, SCF	−2.83	−1.56	−0.03	−5.85	−1.39	−4.06
PP error, SCF+CCSD(T), val	−2.38	0.89	0.16	−1.73	−1.84	−1.99
PP error, SCF+CCSD(T), val+5sp	5.61	−1.82	2.79	−0.43	−1.47	0.65
4f correlation	3.90	6.30	6.77	2.01	4.54	4.39
effect of triples	−37.62	−46.54	−55.55	−67.52	−65.45	−58.61
MRCISD vs CCSD(T)	6.57	0.18	−2.33	−27.50	−25.83	−30.95
SO	0.00	−2.89	−4.49	3.38	−7.38	−30.08

[a] For a detailed explanation, see the text.

TABLE 3: Analysis of Various Contributions to Dissociation Energies D_e (kcal/mol)[a]

	HfO	TaO	WO	ReN	OsN	IrN
basis set effect vtz→CBS	4.80	5.28	5.93	9.00	8.89	8.71
basis set effect wcvtz→CBS	4.45	4.73	5.09	7.70	7.79	7.22
5sp correlation	2.73	1.27	0.52	0.71	0.06	−0.60
PP error, SCF+CCSD(T), val	4.75	2.26	0.74	0.24	−0.71	−0.57
PP error, SCF+CCSD(T), val+5sp	4.92	2.51	1.36	0.91	−0.45	−0.07
4f correlation	1.89	0.86	0.69	0.67	0.33	0.46
SO_{mol}	0.02	5.02	5.18	6.64	9.32	2.57
SO_{at}	−7.84	−10.21	−12.74	0.00	−7.57	−10.38

[a] For a detailed explanation, see the text.

(D_e). It is seen that the effect is of the order of <1 pm for r_e, in all cases leading to a bond length shortening. With core−valence correlation included, it is up to a factor of 2 larger for the early 5d oxides but slightly smaller than that of valence correlation for the late 5d nitrides. Consistent with these changes, ω_e increases toward the basis set limit, by up to ∼15 cm^{-1}, and again, the basis set effect is larger with outer-core−valence correlation included for the earlier 5d elements. For D_e, finally, basis set effects are of the order of ∼5 kcal/mol for the oxides and of ∼10 kcal/mol for the nitrides, leading to an increase of D_e in all cases. Core−valence correlation leaves these effects nearly unchanged for the oxides, while a small decrease can be observed for the nitrides.

3.2. Correlation Effects. Correlation of the metal valence 6s5d orbitals (together with the 2sp shells of nitrogen and oxygen) is indispensable, of course, for a meaningful comparison to experiment. It lengthens r_e by ∼5 pm and reduces ω_e by between 100 and 200 cm^{-1}; see Tables 1 and 2. More subtle but also important is the correlation contribution of the outer-core 5sp shells of the metal atoms. It is primarily of dynamical nature and counteracts that of valence correlation; eventually, it leads to Δr_e values of up to −0.5 pm for the nitrides and of up to −3 pm for the oxides. The corresponding effect on the vibrational frequencies is $\Delta\omega_e \leq 10$ cm^{-1} for the nitrides and $\Delta\omega_e \leq 40$ cm^{-1} for the oxides. For the dissociation energies, outer-core−valence correlation effects are below 1 kcal/mol for the nitrides but tend to increase to 3 kcal/mol for the early oxides.

3.3. Accuracy of PPs. To get information on the reliability of the PPs, we compared PP and all-electron DK3 results with triple-ζ basis sets. It turns out that the deviations for r_e are dominated by SCF effects: While the differences are small (∼0.2 pm) at the end of the row, they become ∼0.5 pm in the middle of the row and increase to ∼2 pm for HfO. This is not unexpected since Hf is the first element following the lanthanides, and the 4f shell is still relatively high in energy: It is by 0.9 E_h lower than the valence 5d and 6s orbitals in the Hf atom and by ∼0.7...0.8 E_h lower than the O 2p-like orbitals in HfO, but it plays the role of a high-lying outer-core shell. In fact, for the Hf atom, the 4f orbitals are higher in energy than the 5p ones by 0.4 E_h, and in the HfO molecule, they heavily mix with the O 2s and Hf 5p orbitals. In this case, as well as in ReN, simple orbital rotation was not sufficient to separate the 4f orbitals from the 5sp ones, and frozen cores taken from the free atoms were used in these two cases. Hence, the frozen-core approximation underlying the PP construction is not fully

valid. In comparison to that, differential correlation effects between PP and AE calculations are rather small, of a few tenths of a pm for r_e; for outer-core−valence correlation, the deviations are <0.1 pm throughout. Note, however, that these statements refer to the case that the correlated space of orbitals is identical in the PP and AE case. They are no longer true, as could have been foreseen, when correlation of the 4*f* shell is included in the AE calculation; see Table 1. Again, the effect is largest at the beginning of the row and reaches nearly 1 pm for HfO. It becomes apparent from this discussion that the early 5d element PPs need corrections, either from AE calculations or from core-polarization potentials (CPP),[29] to provide a reliable description of 4f shell contributions. In total, the AE corrections to the PP bond lengths amount to ∼1, 0.6, and 0.2 pm for HfO, TaO, and WO, respectively, while they are negligible for ReN, OsN, and IrN. Considering ω_e values now, we see (Table 2) that the PP-AE differences are moderate (≤6 cm^{-1}) in all cases, if the 4f shell is kept uncorrelated; correlating it leads to an enhancement of between 2 and 7 cm^{-1}. A similar picture as for r_e evolves from the inspection of the D_e values (Table 3): PP-AE deviations with triple-ζ basis sets increase from 0.1 kcal/mol (IrN) over ∼1 kcal/mol (ReN and WO) to 5 kcal/mol (HfO), the PPs being too attractive, as long as the 4f shell is kept frozen in the AE case; correlation of the 4f shell partly counteracts the PP error, reducing the AE-PP deviation to below 3 kcal/mol for all molecules.

3.4. Multireference Treatment. Correlation of valence and outer-core electrons was done at the CCSD(T) level, as mentioned before. Of course, the question arises whether a single-reference treatment like that is justified for compounds of elements with open d shells. Inspection of the influence of the triple excitations in CCSD(T) on bond lengths and harmonic frequencies shows that the effects are moderate but significant (see Tables 1 and 2). The bond lengths are increased by 1−2 pm, and frequencies are decreased by 40−70 cm^{-1}. Also, the T_1 diagnostics in the CCSD(T) calculations, which are indicators of the importance of multireference character, exhibit values of ∼0.03 and are on the large side. Additional calculations for IrN and OsN with full triples in the coupled-cluster treatment (CCSDT), using cc-pVTZ basis sets, reduced r_e by 0.2 pm and enhanced ω_e by ∼5 cm^{-1}. This is a fairly small effect, indicating the relatively high accuracy of the perturbative triples treatment, but the impact of including connected quadruple excitations (CCSDTQ, cc-pVDZ basis sets) is relatively large: The effect of the latter leads to an enhancement of 0.4−0.5 pm for r_e and to a reduction of ω_e by as much as 25 cm^{-1}. This is perhaps not unexpected given the total magnitude of the triples contributions shown in Tables 1 and 2. To further check on the validity of the CCSD(T) results, we decided to perform multireference CISD calculations, including all metal 6s5d and oxygen/nitrogen 2sp orbitals into the active space, that is, allowing for all possible occupations within this space in the reference wave function and allowing for single and double excitations from the reference wave function into the external space (with a Davidson correction for higher substitutions). As compared to the CCSD(T) results, using a cc-pVTZ basis set in both cases, we observed a bond lengthening of ∼0.5 pm for IrN and OsN and a concomitant increase of ω_e by 25−30 cm^{-1} (see Tables 1 and 2). Effects of similar magnitude were also found for ReN, while only marginal changes of $\Delta r_e < 0.02$ pm and $\Delta\omega_e < 7$ cm^{-1} were obtained in MRCISD calculations for the oxides, with respect to the CCSD(T) ones.

3.5. SO Interaction. The results discussed so far were obtained in scalar-relativistic calculations. To estimate SO corrections to these results, we determined matrix elements of the SO part of the PPs between ground and low-lying excited states, in MRCISD calculations similar to those described in the previous paragraph. The resulting molecular bond length and frequency changes turn out to be largest toward the end of the row (where the multireference character of the wave function is most prominent): for IrN, $\Delta r_e = +0.5$ pm, and $\Delta\omega_e = -30$ cm^{-1}; however, the effects are much smaller at the beginning of the row ($\Delta r_e \leq 0.05$ pm, and $\Delta\omega_e < 5$ cm^{-1}) and remain so for all of the oxides considered and also for ReN.

While SO effects on bond lengths and vibrational frequencies are of only moderate size, this is no longer the case for their contributions to dissociation energies. Here, molecular effects of up to nearly 10 kcal/mol arise; see Table 3. Of course, SO effects are also essential when treating the free ground-state 5d atoms. Experimental SO splittings of ground-state multiplets[30] can be used to estimate SO-induced lowerings of scalar-relativistic atomic ground-state energies; these lowerings are between 0 and 13 kcal/mol. Because the total SO effect on D_e is thus composed of quite large contributions of different sign and, in addition, was determined from different sources, it is probably less accurate than other results of this paper.

3.6. Comparison to Experiment. In Tables 4 and 5, our final results for r_e and ω_e are compared to experiment. This is done in two stages: First, our best scalar-relativistic PP CCSD(T) results, with outer-core correlation and basis set extrapolation, are shown. Second, corrections for multireference contributions, SO interaction, and PP errors are included. It is seen that at the first stage bond lengths are systematically underestimated by 0.75−1.35 pm, while harmonic frequencies are overestimated by 10−80 cm^{-1}. Especially for ω_e, the errors significantly increase for the diatomics with late 5d elements. Including the corrections systematically improves the overall accuracy. Deviations of bond lengths from experiment are now between −0.1 and −0.3 pm (with one exception, WO, where $\Delta r_e = -0.5$ pm).

TABLE 4: Comparison to Experiment for Bond Lengths r_e (pm)[a]

	PP	PP + corrections	exp
HfO	171.225 (−1.090)	172.214 (−0.100)	172.314[b]
TaO	167.870 (−0.865)	168.506 (−0.228)	168.734[c]
WO	164.966 (−0.842)	165.269 (−0.539)	165.807[d]
ReN	163.015 (−0.765)	163.517 (−0.263)	163.780[e]
OsN	160.908 (−0.895)	161.553 (−0.249)	161.802[f]
IrN	159.322 (−1.361)	160.398 (−0.285)	160.683[g]

[a] PP: scalar-relativistic PP CCSD(T) results with CBS-extrapolated (aug-)cc-pwCVnZ basis sets, including metal 5sp correlation. For corrections, cf. Table 1 and the text. Numbers in parentheses are deviations from experiment (exp). [b] Ref 8. [c] Ref 9. [d] Ref 10. [e] Ref 11. [f] Ref 12. [g] Ref 13.

TABLE 5: Comparison to Experiment for Harmonic Wavenumbers ω_e (cm^{-1})[a]

	PP	PP + corrections	exp
HfO	981.49 (7.40)	986.35 (12.26)	974.09[b]
TaO	1038.74 (9.83)	1044.15 (15.24)	1028.91[c]
WO	1087.82 (22.20)	1084.98 (19.36)	1065.62[d]
ReN	1163.53	1141.85	1121.52[e]
OsN	1193.24 (45.29)	1166.04 (18.09)	1147.95[f]
IrN	1203.90 (77.72)	1146.61 (20.43)	1126.18[g]

[a] PP: scalar-relativistic PP CCSD(T) results with CBS-extrapolated (aug-)cc-pwCVnZ basis sets, including metal 5sp correlation. For corrections, cf. Table 2 and the text. Numbers in parentheses are deviations from experiment (exp). [b] Ref 8. [c] Ref 9. [d] Ref 10. [e] Ref 11; $\Delta G_{1/2}$. [f] Ref 12. [g] Ref 13.

TABLE 6: Comparison to Experiment for Dissociation Energies D_e (kcal/mol)[a]

	PP	PP + corrections	exp
HfO	205.67	194.82	191.6 ± 3[b]
TaO	194.10	187.26	191.0 ± 3[b]
WO	178.19	169.96	160.6 ± 10[b], 172 ± 17[c]
ReN	125.34	131.74	
OsN	135.88	138.41	
IrN	134.51	127.23	144.1[d]

[a] PP: scalar-relativistic PP CCSD(T) results with CBS-extrapolated (aug-)cc-pwCVnZ basis sets, including metal 5sp correlation. For corrections, cf. Table 3 and the text. Experimental data are D_{298}^0 values, if not indicated otherwise. [b] Ref 34. [c] Ref 35. [d] Ref 13; D_e was estimated from vibrational constants.

Also, harmonic frequencies are of much more uniform quality, with $\Delta\omega_e$ exhibiting values between +10 and +20 cm^{-1}. Further improvement is probably not easily possible, since the remaining bond length errors are in a regime where relativistic two-electron Breit terms for the heavy atoms (implicitly included in the PP calculations but not accounted for in the AE DK3 calculations) may become non-negligible.[32,33]

Our results for D_e are summarized in Table 6. Here, the corrections to the CBS-extrapolated CCSD(T) results with the scalar-relativistic PPs (first column) include corrections for PP errors and for atomic as well as molecular SO contributions (second column). As mentioned above, the SO effects and therefore also the final results are probably of inferior quality to those obtained for r_e and ω_e. Moreover, there are only few experimental data (partly with large error bars) to compare.

It should be noted that for part of the molecules considered in this paper (WO, OsN, and IrN), accurate ab initio results by Liévin and co-workers are available in the literature.[10,12,31] These calculations were performed at the MRCISD level, correlating the metal 5d and 6s shells and using the previous generation of our Wood−Boring based energy-consistent PPs in conjunction with triple-ζ quality basis sets. The resulting bond lengths (167.2, 162.7, and 160.9 pm for WO, OsN, and IrN, respectively) and corresponding harmonic wavenumbers (1050, 1146, and 1161 cm^{-1}) deviate from experiment by <1.5 pm and <40 cm^{-1} only. According to our present study, this good agreement is partly fortuitous. On the other hand, the calculations of Liévin and co-workers address not only ground states but also low-lying excited states. Interestingly, their averaging over ground and excited states for determining CASSCF orbitals leads to a quite substantial multireference character for the ground states, with weights of the CASSCF references in the MRCISD wave functions of around 80%. These weights are considerably smaller than in our case (~90%) where the CASSCF references were optimized for ground states exclusively. Let us finally mention MRACPF (averaged coupled-pair functional) calculations for TaO with our older Wood−Boring-adjusted PPs,[6] which also yielded results in very good agreement with experiment (r_e = 169.1 pm, ω_e = 1023 cm^{-1}, and D_e = 176.9 kcal/mol).

4. Investigation of Pt_2

As the Pt atom exhibits a $5d^96s^1$ ground-state orbital occupation, the number of possible low-lying molecular states is much larger than in the case of the palladium dimer, Pd_2. In the latter case, the molecular $^3\Sigma_u^+$ ground state can be rationalized, in a simplified description, as a combination of a $4d^{10}$ ground-state atom and a partner atom promoted to $4d^95s^1$;[37] in a molecular picture, this means that 19 electrons populate the 10 molecular orbitals that are linear combinations of atomic 4d orbitals and one electron occupies the bonding σ_g orbital that results from the linear combination of the atomic 5s orbitals. For Pt_2, the combination of two $5d^96s^1$ ground-state atoms leads to the more complicated situation where only 18 electrons occupy the 10 molecular orbitals that are linear combinations of the atomic 5d orbitals and consequently to more states that are close in energy. Table 7 lists the states that we investigated and their orbital occupations. A number of states are accessible to CCSD(T) calculations as they are either high-spin states ($^3\Sigma_g^-$, $^3\Pi_u$, $^3\Delta_g$, $2^3\Sigma_u^+$, and $^3\Delta_u$) or closed-shell states ($^1\Sigma_g^+$); for the other high-spin states ($^3\Phi_u$ and $2^3\Pi_u$ as well as $^3\Gamma_u$ and $^3\Sigma_u^+$), a single-reference treatment investigates the average over both states as both states are identical in orbital occupation and multiplicity. Still, this treatment leads to reliable results as the T_1 diagnostic remains ~0.025 for the larger basis sets; for the cc-pwCVDZ basis set, the T_1 diagnostic becomes larger than 0.03, and this basis set is too small to accurately describe states with angular momenta as high as Λ = 4 (cf. Figure 1−3). In all CI calculations necessary for the simulation of coupled-cluster energies for those states which cannot directly be treated by CCSD(T) calculations, the coefficients of the SCF reference functions remain larger than 0.92; this observation also supports the validity of our single-reference treatment of Pt_2.

TABLE 7: Orbital Occupations and Resulting Scalar-Relativistic States for Pt_2 That Have Been Investigated in This Work[a]

orbital occupation	states
$1\sigma_g^2 1\pi_u^4 1\delta_g^4 1\delta_u^4 1\pi_g^2 2\sigma_g^2 1\sigma_u^2$	$^3\Sigma_g^-$, $^1\Delta_g$, $2^1\Sigma_g^+$
$1\sigma_g^2 1\pi_u^4 1\delta_g^4 1\delta_u^4 1\pi_g^3 2\sigma_g^2 1\sigma_u^1$	$^3\Pi_u$, $^1\Pi_u$
$1\sigma_g^2 1\pi_u^4 1\delta_g^4 1\delta_u^4 1\pi_g^4 2\sigma_g^2$	$^1\Sigma_g^+$
$1\sigma_g^2 1\pi_u^4 1\delta_g^4 1\delta_u^3 1\pi_g^3 2\sigma_g^2 1\sigma_u^2$	$^3\Phi_u$, $2^3\Pi_u$, $^1\Phi_u$, $2^1\Pi_u$
$1\sigma_g^2 1\pi_u^4 1\delta_g^4 1\delta_u^3 1\pi_g^4 2\sigma_g^2 1\sigma_u^1$	$^3\Delta_g$, $2^1\Delta_g$
$1\sigma_g^2 1\pi_u^4 1\delta_g^3 1\delta_u^3 1\pi_g^4 2\sigma_g^2 1\sigma_u^2$	$^3\Gamma_u$, $^3\Sigma_u^+$, $^1\Sigma_u^-$
$1\sigma_g^2 1\pi_u^4 1\delta_g^4 1\delta_u^4 1\pi_g^4 2\sigma_g^1 1\sigma_u^1$	$2^3\Sigma_u^+$, $^1\Sigma_u^+$
$1\sigma_g^2 1\pi_u^4 1\delta_g^3 1\delta_u^4 1\pi_g^4 2\sigma_g^2 1\sigma_u^1$	$^3\Delta_u$

[a] The specified molecular orbitals are combinations of atomic 5d and 6s orbitals.

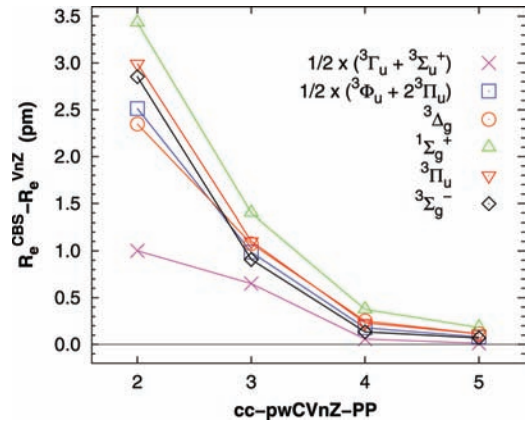

Figure 1. Pt_2: The equilibrium distance r_e as a function of basis set size. Results from CCSD(T) calculations using the cc-pwCVnZ basis set series.

The CCSD(T) results at the cc-pwCVnZ basis set limit are shown in Table 8 in connection with the deviations of the PP results from all-electron results at the cc-pwCVTZ level. The latter amount to only ±0.2−0.3 pm in r_e and ~1 cm^{-1} in ω_e and thus are as small as for the nitrides discussed earlier. The vertical excitation energies T_e show larger errors of ~200 cm^{-1}, which may be due to the fact that these energies are differences between two values that may have errors with different signs;

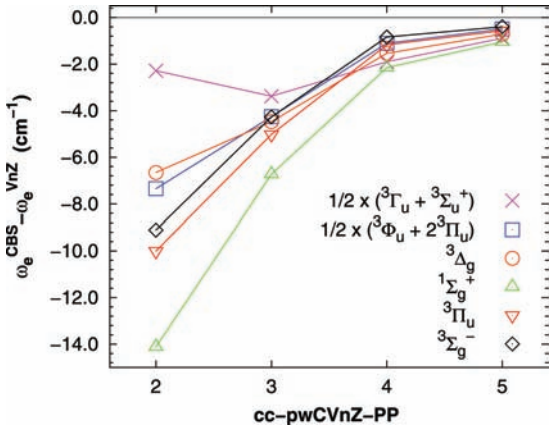

Figure 2. Pt_2: The harmonic wavenumbers ω_e as a function of basis set size. Results from CCSD(T) calculations using the cc-pwCVnZ basis set series.

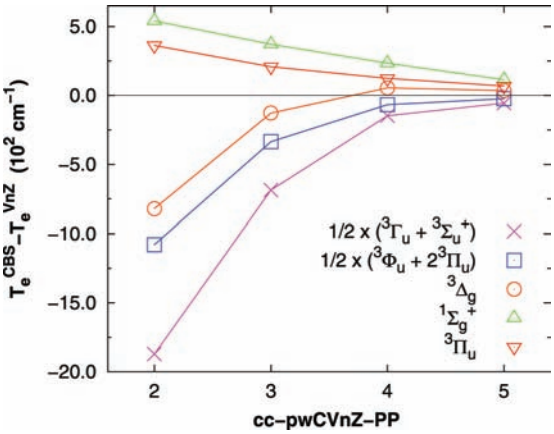

Figure 3. Pt_2: The term energies T_e as a function of basis set size. Results from CCSD(T) calculations using the cc-pwCVnZ basis set series.

TABLE 8: Scalar-Relativistic CCSD(T) Results at the cc-pwCVnZ Basis Set Limit for the Spectroscopic Constants of the Lowest Electronic States of Pt_2[a]

state	r_e	ω_e	T_e
$^3\Sigma_g^-$	229.36 (−0.28)	252.57 (0.21)	0 (0)
$^3\Pi_u$	230.47 (−0.20)	246.88 (0.19)	1515 (71)
$^1\Sigma_g^+$	232.24 (0.14)	236.54 (−1.09)	3531 (342)
1/2 × ($^3\Phi_u$ + 2$^3\Pi_u$)	235.34 (−0.33)	230.24 (1.10)	4916 (196)
$^3\Delta_g$	236.08 (−0.26)	228.63 (0.87)	4807 (92)
1/2 × ($^3\Gamma_u$ + $^3\Sigma u$ +)	248.60 (−0.11)	198.98 (0.02)	5944 (227)
$2^3\Sigma_u^+$	245.51 (0.05)	200.31 (−0.28)	6669 (180)
$^3\Delta_u$	243.61 (−0.31)	209.40 (1.05)	9350 (140)

[a] The deviations of the PP results from all-electron DK2 results at the cc-pwCVTZ level are shown in parentheses. Values are given in pm for r_e and cm^{-1} for ω_e and T_e.

still, the differences between PP and AE results are smaller than the basis set effects for T_e, as going from the triple-ζ level to the CBS can lead to changes of up to ±600...700 cm^{-1}. Table 9 shows the CCSD(T) or simulated CCSD(T) (cf. section 2) results for all states; it is clear that an assignment of the experimental data ($\Omega = 0$, $r_0 = 233.297$ pm, $\omega_e = 222.46$ cm^{-1})[38,39] to a scalar-relativistic state cannot be accomplished from the scalar-relativistic data alone as the differences between the scalar-relativistic states are small.

The results for the lowest relativistic levels are shown in Table 10. The ground-state results for r_e and ω_e differ from the experimental values only by 3 pm and 1 cm^{-1}, respectively,

TABLE 9: Scalar-Relativistic CCSD(T) Results at the cc-pwCVnZ Basis Set Limit for the Spectroscopic Constants of the Lowest Electronic States of Pt_2[a]

state	r_e	ω_e	T_e
$^3\Sigma_g^-$	229.4	252.6	0
$^3\Pi_u$	230.5	246.9	1515
$^1\Sigma_g^+$	232.2	236.5	3531
$^3\Phi_u$	235.3	230.6	3875
$^1\Pi_u$	230.2	248.1	4514
$^3\Delta_g$	236.1	228.6	4807
$^1\Delta_g$	229.7	250.1	5383
$2^3\Pi_u$	235.4	229.7	5909
$^3\Gamma_u$	248.6	199.0	5940
$^3\Sigma_u^+$	248.6	199.0	5947
$2^3\Sigma_u^+$	245.5	200.3	6669
$^1\Sigma_u^-$	248.6	196.0	6766
$^1\Phi_u$	235.7	228.4	8877
$^3\Delta_u$	243.6	209.4	9350
$2^1\Sigma_g^+$	230.0	247.4	10427
$2^1\Pi_u$	235.9	227.3	11031
$2^1\Delta_g$	237.5	221.5	12020
$^1\Sigma_u^+$	243.0	205.9	20200

[a] For low-spin open shell states or states with identical orbital occupation and multiplicity, CCSD(T) results have been simulated by an energetic shift of CISD results (see the text). Values are given in pm for r_e and cm^{-1} for ω_e and T_e.

TABLE 10: Spectroscopic Constants of the Lowest SO Coupled States of Pt_2 from MRCISD Calculations Using the cc-pVQZ Basis Set[a]

state	r_e	ω_e	T_e
4_u (89% $^3\Phi_u$, 11% $^3\Gamma_u$)	236.4	221.6	0
5_u (99% $^3\Gamma_u$)	248.5	198.9	1706
0_g^+ (88% $^3\Sigma_g^-$, 12% $2^1\Sigma_g^+$)	228.3	273.6	2156
0_u^- (48% $^1\Sigma_u^-$, 45% $^3\Sigma_u^+$)	248.7	198.2	2161
exp	233.3[b]	222.5[c]	0

[a] The diagonal elements of the SO matrix have been substituted by the results at the cc-pwCVnZ basis set limit. Values are given in pm for r_e and cm^{-1} for ω_e and T_e. [b] r_0; ref 38. [c] Ref 39.

and are therefore very satisfactory; however, a major disagreement arises for the symmetry of the ground states. The calculations result in a 4_u ground state, whereas the experimental investigations indicate a 0_g^+ or 0_u^- ground state.[38,39] The lowest SO coupled state originates mainly from the scalar-relativistic $^3\Phi_u$ state, although the latter is the fourth to lowest scalar-relativistic state. The strong lowering of the relativistic level is mainly due to the coupling between the two space degenerate $^3\Phi_u$ states, which is as large as ∼6300 cm^{-1} near the equilibrium distance of this level. The 5_u and the 0_u^- levels exhibit even larger SO couplings of ∼7900 cm^{-1} (between both space degenerate $^3\Gamma_u$ states) and of ∼7300 cm^{-1} (between the $^1\Sigma_u^-$ and the $^3\Sigma_u^+$ states), respectively; for the 0_g^+ level, the coupling between the $^3\Sigma_g^-$ and the $2^1\Sigma_g^+$ states is smaller and amounts to ∼4300 cm^{-1} near the equilibrium geometry. For all cases, the large SO couplings arise between states that have identical orbital occupation (cf. Table 7). Although the SO couplings are as large as the term energies between scalar-relativistic states, the three lowest relativistic levels are dominated by one scalar-relativistic state each; this shows that an investigation starting from one-component orbitals is in principle applicable, even if a two-component investigation may be desirable. An earlier ab initio investigation[40] used basis sets of triple-ζ size in first-order CI calculations; although the resulting 0_g^+ ground state showed the right symmetry, the results for r_e (245.6 pm) and ω_e (189 cm^{-1}) deviated by 12 pm and 33 cm^{-1} from the experimental

data. A relativistic density functional study[41] reproduced the experimental data much better with deviations of 1−3 pm in r_e and 3−15 cm^{-1} in ω_e using different relativistic density functionals; in that study, the ground state was found to be a closed shell system. This disagrees with our results as the closed shell $^1\Sigma_g^+$ state does not interact very strongly with other states and thus does not result in a low-lying relativistic level after the inclusion of SO coupling.

5. Conclusion

Benchmark calculations with newly developed MCDHF adjusted energy-consistent PPs and series of correlation-consistent polarized valence and core−valence n-ζ basis sets have been performed for the diatomics HfO, TaO, WO, ReN, OsN, and IrN. At the CBS limit, scalar-relativistic CCSD(T) calculations including metal 5sp core correlation consistently underestimate bond lengths by ∼1 pm and overestimate harmonic wavenumbers by ∼30 cm^{-1}. With corrections for SO effects, multireference treatment, and PP errors, the deviations can be reduced to 0.3 pm for r_e and 17 cm^{-1} for ω_e. In particular, contributions from correlating the closed 4f shell are non-negligible for the early 5d elements.

An investigation of Pt_2 showed that SO couplings between states of identical orbital occupation are of the same order of magnitude as the term energies between scalar-relativistic states. Therefore, the investigation of Pt_2 requires extensive calculations or should be two-component from the onset. The experimental ground-state spectroscopic data could be reproduced in PP calculations with deviations of 3 pm in r_e and 1 cm^{-1} in ω_e. A disagreement in the symmetry of the ground state between theory and experiment may advise further theoretical and experimental studies.

References and Notes

(1) Dolg, M. In *Relativistic Electronic Structure Theory—Fundamentals, Theoretical and Computational Chemistry*; Schwerdtfeger, P., Ed.; Elsevier: Amsterdam, 2003; Vol. 11.
(2) Pyykkö, P.; Stoll, H. In *R.S.C. Specialist Periodical Reports: Chemical Modelling, Applications and Theory*; Hinchliffe, A., Ed.; RSC: London, 2000, Vol. 1.
(3) Stoll, H.; Metz, B.; Dolg, M. *J. Comput. Chem.* **2002**, *23*, 767.
(4) Peterson, K. A.; Figgen, D.; Dolg, M.; Stoll, H. *J. Chem. Phys.* **2007**, *126*, 124101.
(5) Figgen, D.; Peterson, K. A.; Dolg, M.; Stoll, H. J. *Chem. Phys.*, **2009**, *130*, 164108.
(6) Dolg, M.; Stoll, H.; Preuss, H.; Pitzer, R. M. *J. Phys. Chem.* **1993**, *97*, 5852.
(7) Peterson, K. A. *J. Chem. Phys.* **2003**, *119*, 11099.
(8) Lesarri, A.; Suenram, R. D.; Brugh, D. *J. Chem. Phys.* **2002**, *117*, 9651.
(9) Ram, R. S.; Bernath, P. F. *J. Mol. Spectrosc.* **1998**, *191*, 125.
(10) Ram, R. S.; Liévin, J.; Li, G.; Hirao, T.; Bernath, P. F. *Chem. Phys. Lett.* **2001**, *343*, 437.
(11) Ram, R. S.; Bernath, P. F.; Balfour, W. J.; Cao, J.; Qian, C. X. W.; Rixon, S. J. *J. Mol. Spectrosc.* **1994**, *168*, 350.
(12) Ram, R. S.; Liévin, J.; Bernath, P. F. *J. Chem. Phys.* **1999**, *111*, 3449.
(13) Ram, R. S.; Bernath, P. F. *J. Mol. Spectrosc.* **1999**, *193*, 363.
(14) Dunning, T. H., Jr. *J. Chem. Phys.* **1989**, *90*, 1007.
(15) Kendall, R. A.; Dunning, T. H., Jr.; Harrison, R. J. *J. Chem. Phys.* **1992**, *96*, 6796.
(16) Raghavachari, K.; Trucks, G. W.; Pople, J. A.; Head-Gordon, M. *Chem. Phys. Lett.* **1989**, *156*, 479.
(17) Hampel, C.; Peterson, K.; Werner, H.-J. *Chem. Phys. Lett.* **1992**, *190*, 1.
(18) Knowles, P. J.; Hampel, C.; Werner, H.-J. *J. Chem. Phys.* **1993**, *99*, 5219. Erratum: *J. Chem. Phys.* **2000**, *112*, 3106.
(19) Deegan, M. J. O.; Knowles, P. J. *Chem. Phys. Lett.* **1994**, *227*, 321.
(20) Werner, H.-J.; Knowles, P. J. *J. Chem. Phys.* **1985**, *82*, 5053.
(21) Knowles, P. J.; Werner, H.-J. *Chem. Phys. Lett.* **1985**, *115*, 259.
(22) Werner, H.-J.; Knowles, P. J. *J. Chem. Phys.* **1988**, *89*, 5803.
(23) Knowles, P. J.; Werner, H.-J. *Chem. Phys. Lett.* **1988**, *145*, 514.
(24) Langhoff, S. R.; Davidson, E. R. *Int. J. Quantum Chem.* **1974**, *8*, 61.
(25) MRCC, a string-based quantum chemical program suite written by Kállay, M. See http://mrcc.hu. See also Kállay, M.; Surján, P. R. *J. Chem. Phys.* **2001**, *115*, 2945. Kállay, M.; Szalay, P. G.; Surján, P. R. *J. Chem. Phys.* **2002**, *117*, 980.
(26) Hess, B. A. *Phys. Rev. A* **1986**, *33*, 3742.
(27) Wolf, A.; Reiher, M.; Hess, B. A. *J. Chem. Phys.* **2002**, *117*, 9215.
(28) MOLPRO, version 2008.1, a package of ab initio programs: Werner, H.-J.; Knowles, P. J.; Lindh, R.; Manby, F. R.; Schütz, M.; and others; see http://www.molpro.net.
(29) Nicklass, A.; Stoll, H. *Mol. Phys.* **1995**, *86*, 317.
(30) Moore, C. E. *Atomic Energy Levels*; Circular 467; National Bureau of Standards: Washington, DC, 1958; Vol. 3.
(31) Ram, R. S.; Liévin, J.; Bernath, P. F. *J. Mol. Spectrosc.* **1999**, *197*, 133.
(32) Faegri, K., Jr.; Visscher, L. *Theor. Chem. Acc.* **2001**, *105*, 265.
(33) Visser, O.; Visscher, L.; Aerts, P. J. C. *Theor. Chem. Acc.* **1992**, *81*, 405.
(34) Pedley, J. B.; Marshall, E. M. *J. Phys. Chem. Ref. Data* **1984**, *12*, 967.
(35) Blagojevic, V.; Koyanagi, G. K.; Lavrov, V. V.; Orlova, G.; Bohme, D. K. *Chem. Phys. Lett.* **2004**, *389*, 303.
(36) Helgaker, T.; Klopper, W.; Koch, H.; Noga, J. *J. Chem. Phys.* **1997**, *106*, 9639.
(37) Figgen, D.; Peterson, K. A.; Stoll, H. *J. Chem. Phys.* **2008**, *128*, 034110.
(38) Fabbi, J. C.; Langenberg, J. D.; Costello, Q. D.; Morse, M. D.; Karlsson, L. *J. Chem. Phys.* **2001**, *115*, 7543.
(39) Airola, M. B.; Morse, M. D. *J. Chem. Phys.* **2002**, *116*, 1313.
(40) Balasubramanian, K. *J. Chem. Phys.* **1987**, *87*, 6573.
(41) Anton, J.; Jacob, T.; Fricke, B.; Engel, E. *Phys. Rev. Lett.* **2002**, *89*, 213001.

JP903543F